

MIT Open Access Articles

Quantifying kinetic uncertainty in turbulent combustion simulations using active subspaces

The MIT Faculty has made this article openly available. **Please share** how this access benefits you. Your story matters.

Citation: Ji, Weiqi et al. "Quantifying kinetic uncertainty in turbulent combustion simulations using active subspaces." Proceedings of the Combustion Institute, vol. 37, no. 2, 2019, pp. 2175-2182 © 2019 The Author(s)

As Published: 10.1016/J.PROCI.2018.06.206

Publisher: Elsevier BV

Persistent URL: <https://hdl.handle.net/1721.1/126335>

Version: Author's final manuscript: final author's manuscript post peer review, without publisher's formatting or copy editing

Terms of use: Creative Commons Attribution-NonCommercial-NoDerivs License





ELSEVIER

Available online at www.sciencedirect.com

ScienceDirect

Proceedings of the Combustion Institute 000 (2018) 1–8

Proceedings
of the
Combustion
Institutewww.elsevier.com/locate/proci

Quantifying kinetic uncertainty in turbulent combustion simulations using active subspaces

Weiqi Ji^a, Zhuyin Ren^{a,*}, Youssef Marzouk^b, Chung K. Law^{a,c}^a Center for Combustion Energy, Tsinghua University, Beijing 100084, China^b Massachusetts Institute of Technology, Cambridge, MA 02139, USA^c Department of Mechanical and Aerospace Engineering, Princeton University, Princeton, NJ 08544, USA

Received 1 December 2017; accepted 26 June 2018

Available online xxx

Abstract

Uncertainty quantification in expensive turbulent combustion simulations usually adopts response surface techniques to accelerate Monte Carlo sampling. However, it is computationally intractable to build response surfaces for high-dimensional kinetic parameters. We employ the active subspaces approach to reduce the dimension of the parameter space, such that building a response surface on the resulting low-dimensional subspace requires many fewer runs of the expensive simulation, rendering the approach suitable for various turbulent combustion models. We demonstrate this approach in simulations of the Cabra H₂/N₂ jet flame, propagating the uncertainties of 21 kinetic parameters to the liftoff height. We identify a one-dimensional active subspace for the liftoff height using 84 runs of the simulations, from which a response surface with a one-dimensional input is built; the probability distribution of the liftoff height is then characterized by evaluating a large number of samples using the inexpensive response surface. In addition, the active subspace provides a global sensitivity metric for determining the most influential reactions. Comparison with autoignition tests reveals that the sensitivities to the HO₂-related reactions in the Cabra flame are promoted by the diffusion processes. The present work demonstrates the capability of active subspaces in quantifying uncertainty in turbulent combustion simulations and provides physical insights into the flame via the active subspace-based sensitivity metric.

© 2018 The Combustion Institute. Published by Elsevier Inc. All rights reserved.

Keywords: Uncertainty quantification; Active subspaces; Turbulent lifted flames; Autoignition

1. Introduction

Simulation of turbulent combustion is usually associated with uncertainties from the turbulent combustion model, the chemical kinetic model, the boundary conditions, etc. For example, detailed ki-

netic models for hydrocarbon fuels have a large set of elementary reactions with many rate constants which inevitably contain uncertainties. It remains an open question as whether the uncertainties in kinetic models can be small enough to satisfy the needs of combustion simulations with prescribed accuracy requirements.

Uncertainty quantification (UQ) provides a set of methods to address the above question by

* Corresponding author.

E-mail address: zhuyinren@tsinghua.edu.cn (Z. Ren).

<https://doi.org/10.1016/j.proci.2018.06.206>

1540-7489 © 2018 The Combustion Institute. Published by Elsevier Inc. All rights reserved.

quantifying the uncertainties in the models as well as the predictions, and usually consists of two steps. Take the kinetic uncertainty as an example. The first step, the so-called *inverse* problem [1–3], aims at quantifying the distribution of the model parameters based on experimental data under simplified flow conditions, such as the ignition delay time. The second step, usually referred to as the *forward* problem, with the combustion simulation being called the *forward model*, aims at quantifying the uncertainty in the predictions by propagating the above model uncertainties through combustion forward models. During this step, a large number of samples are drawn from the distribution of the model parameters characterized in the first step. Each sample corresponds to a set of model parameters, say the pre-factor A in the reaction mechanism, and the *forward model* is evaluated once for each sample. Consequently the statistics of the predictions from all of the samples can lead to the uncertainty in the prediction, such as its uncertainty interval.

The *forward* problem has been studied for simple combustion problems [4–7], such as the 0-D auto-ignition and the 1-D flame propagation. Most of the cited works employ non-intrusive methods with Monte Carlo (MC) method or its variation. Due to the slow convergence of MC, a large number of samples are required to reach convergence. To alleviate this computational challenge, various response surface techniques [7,8] have been adopted in conjunction with MC, in which one uses a few carefully selected runs of the expensive model to construct a cheaper response surface that is subsequently sampled for MC. However, building response surfaces requires a large number of runs of the expensive model when the number of input parameters is large. For high dimensional kinetic parameters, various methods have been used to reduce the dimension of the input parameter space. For example, local sensitivity analysis and screening methods have been used in [1,9] to identify the input parameters that contribute most to the uncertainties in the outputs. Subsequent response surface construction will then only involve these important parameters and requires much fewer runs of the expensive model.

The present work focuses on the *forward* problem in turbulent combustion, in which the number of affordable simulations is more severely limited since it can take days to weeks for each sample. Recently, the active subspace (AS) dimension reduction method developed by Constantine et al. [10] has attracted considerable attention for UQ applications, and has been successfully applied to the simulations of autoignition and laminar flame speeds [11], and the turbulent combustion simulation of hypersonic scramjet engines [12]. Unlike the standard sensitivity analysis that identifies the important individual input parameters, the AS approach identifies the important directions in

the input parameter space determined in terms of linear combinations of the input parameters. Since the direction is not constrained to be aligned with the canonical basis, the AS approach can lead to further dimension reduction. In [11], the AS method identified one-dimensional structure in the map from rate constants to the ignition delay time for hydrogen/air, methane/air mixtures and five-dimensional structure for dimethyl ether/air mixture under test conditions. In [12], the AS method identified one-dimensional structure in the map from seven input parameters of the operating conditions, such as the angle of attack and turbulence intensity, to the scramjet performance; thus the response surface of a single active variable derived from the seven inputs can be constructed. The total cost is much less than directly building a response surface of seven inputs. It also helps to understand and improve models by better visualizing the map from the high-dimensional inputs to outputs. As a byproduct, the active subspace also reveals the most sensitive parameters for the quantity of interest (QoI). Note that other dimension reduction approaches have also been exploited for turbulent combustion simulations. For example, Mueller et al. [13] developed a dimension reduction algorithm for flamelet-like models by decoupling the uncertainties in the flamelet table induced by kinetic uncertainty from the flow field. However, the algorithm is limited to flamelet-like models and the uncertainties induced by kinetic models. The AS approach is more general and it is suitable for propagating kinetic uncertainty as well as other types of uncertainty sources in the context of various turbulent combustion models.

In this work, the active subspace method is for the first time demonstrated for propagating high dimensional kinetic uncertainty in turbulent combustion simulations; specifically, it is used to propagate the uncertainties in 21 rate constants to the liftoff height in the Cabra H_2/N_2 jet flame [14]. In the following, we shall first introduce the active subspace method, and then apply it to the Cabra flame simulations.

2. Kinetic uncertainty and active subspace

Following previous works [7,11], the rate constants are presumed to be independent lognormal distributions, and are centered and normalized as x_j , which follows the standard normal distribution,

$$x_j = \frac{\ln k_j/k_{j0}}{\frac{1}{3} \ln UF_j} \sim N(0, 1), j = 1, \dots, d, \quad (1)$$

where k_j is the j th reaction rate coefficient, k_{j0} and UF_j are its nominal value and uncertainty factor. The number of elemental reactions is denoted as d , which is also the number of input parameters. The simulation inputs are then represented as a

d -dimensional random vector $\mathbf{x} = [x_1, \dots, x_d]^T$. We denote the distribution of \mathbf{x} as π_x . The deterministic forward combustion model map the inputs to the QoIs, and the map to a specific QoI is denoted as a function $f(\mathbf{x})$.

The active subspace methodology is detailed in [10] with algorithms, a rigorous error analysis, and demonstrations. Here we simply state the basic concepts. The AS method seeks an r -dimensional subspace in the d -dimensional parameter space that describes most of the variation of f . The idea is to find a low-dimensional approximation of f as

$$f(\mathbf{x}) \approx g(\mathbf{x}_r), \quad \mathbf{x}_r = \mathbf{S}^T \mathbf{x}, \quad (2)$$

where g is a function of the r -dimensional input \mathbf{x}_r with $r < d$, and \mathbf{S} is an orthogonal matrix of size $d \times r$. The active subspace is defined as $\text{span}\{\mathbf{S}\}$. One way to identify the active subspace is to perform an eigenvalue decomposition of the matrix \mathbf{C} , defined as the expectation of the outer product of the gradient ∇f with itself, i.e.,

$$\mathbf{C} = \int \nabla f(\mathbf{x}) \nabla f(\mathbf{x})^T \pi_x(\mathbf{x}) d\mathbf{x} = \mathbf{W} \mathbf{\Lambda} \mathbf{W}^T. \quad (3)$$

Note that \mathbf{C} is symmetric, positive semi-definite, and of size $d \times d$. The unitary matrix \mathbf{W} consists of the d eigenvectors $\mathbf{w}_1, \dots, \mathbf{w}_d$ and $\mathbf{\Lambda}$ is a diagonal matrix whose components are the eigenvalues $\lambda_1 \dots \lambda_d$, sorted in descending order. If there is a gap in the eigenvalues, meaning $\lambda_r \gg \lambda_{r+1}$, then the function f varies mostly along the first r eigenvectors and is almost constant along the rest of the eigenvectors. The first r eigenvectors are selected as active directions, i.e., $\mathbf{S} \equiv [\mathbf{w}_1, \dots, \mathbf{w}_r]$; and its complement $\text{span}\{\mathbf{w}_{r+1}, \dots, \mathbf{w}_d\}$ is identified as the inactive subspace. Then one can build a response surface, $\text{RS}(\mathbf{x}_r)$, with \mathbf{x}_r as input, and it is chosen as the function g , i.e., $f(\mathbf{x}) \approx g(\mathbf{x}_r) = \text{RS}(\mathbf{x}_r)$.

The matrix \mathbf{C} can be approximated by MC simulations [10]. The number of runs M of the forward model required depends on how the gradient of f is evaluated, as discussed next.

- (I) In the first scenario, f and its gradient are evaluated simultaneously. Constantine et al. [10] have shown that M increases logarithmically with d , i.e., $M = \alpha \beta \log(d)$. The constant α is the over-sampling factor and is recommended to be between 2 and 10, and β is the largest dimension of the subspace allowed in the subsequent building of the response surface.
- (II) In the second scenario, since derivatives with respect to the kinetic parameters are often not available in legacy combustion codes, the gradients are estimated via finite difference methods and the evaluation of gradients in general takes d runs of the forward model. Thus M will scale with $d \log(d)$, i.e., $M = \alpha \beta d \log(d)$.
- (III) In the third scenario, f is approximately linear with the inputs over the entire input

space, e.g., the integrated exit pressure with respect to the seven inputs in the scramjet simulation [12]. Then, the function has a one-dimensional active subspace, which can be estimated by global linear fitting through ordinary least square (OLS) [10], i.e.,

$$f(\mathbf{x}) = \mathbf{b}^T \mathbf{x} + b_0. \quad (4)$$

The active direction is given by $\mathbf{w}_1 = \mathbf{b}^T / \|\mathbf{b}\|_2$. For such a case, M linearly increases with d , i.e., $M = \alpha d$.

In all scenarios, the error in the estimated eigenvalues and eigenvectors due to insufficient number of runs can be estimated with bootstrapping [12], in which M samples are resampled with replacement for hundreds of times from the runs already evaluated. Then eigen-decomposition is performed for each time of the resampling. The lower and upper bounds of the active subspace provide a good approximation to the error bounds in the computed active subspace. Once the active subspace is identified, various response techniques, such as polynomial fitting, Polynomial Chaos Expansion (PCE) [7] and High Dimensional Model Representation (HDMR) [8], can be readily applied to the low-dimensional active subspace. Depending on the degree of nonlinearity and coupling, PCE and HDMR are suitable for moderate dimensions of the input parameter space.

The entire workflow for propagating the kinetic uncertainty to the QoI in turbulent combustion simulation will be: (1) Estimate the active subspace based on a small number, M , of samples drawn from π_x . The function f and its gradient for each sample are evaluated by performing expensive simulations. (2) Build the response surface $\text{RS}(\mathbf{x}_r)$ to the low-dimensional variable \mathbf{x}_r . (3) Estimate the distribution of the QoI by evaluating a large number, N , of the samples drawn from π_x . The function f is acquired via the cheap response surface $\text{RS}(\mathbf{x}_r)$.

It is worth noting that other dimension reduction methods, such as the basis adaptation method [15], could also be applied, especially if the distribution π_x is non-Gaussian and sampling from it is difficult. A review of the relationship between the active subspace method and other subspace methods is given in [10]. Comparisons among different methods in the context of combustion simulations merit further studies.

As a byproduct, the active subspace also reveals the global sensitivity of the QoI to the inputs [16], i.e., large components of the active direction correspond to the influential parameters. In addition, the active direction provides information on how the kinetic parameters are coupled with each other.

3. TPDF simulations of turbulent lifted jet flames

The Cabra flame [14], which is a turbulent jet flame of H_2/N_2 issued into a hot co-flow of lean

Table 1
The uncertainty factor for each elementary reaction in the Li mechanism.

No.	Reaction	UF	No.	Reaction	UF
1	$\text{H} + \text{O}_2 \rightleftharpoons \text{O} + \text{OH}$	1.5	12	$\text{HO}_2 + \text{O} \rightleftharpoons \text{O}_2 + \text{OH}$	1.2
2	$\text{O} + \text{H}_2 \rightleftharpoons \text{H} + \text{OH}$	1.3	13	$\text{HO}_2 + \text{OH} \rightleftharpoons \text{H}_2\text{O} + \text{O}_2$	3
3	$\text{H}_2 + \text{OH} \rightleftharpoons \text{H}_2\text{O} + \text{H}$	2	14	$\text{HO}_2 + \text{HO}_2 \rightleftharpoons \text{H}_2\text{O}_2 + \text{O}_2$	2.5
4	$\text{O} + \text{H}_2\text{O} \rightleftharpoons \text{OH} + \text{OH}$	1.5	15	$\text{HO}_2 + \text{HO}_2 \rightleftharpoons \text{H}_2\text{O}_2 + \text{O}_2$	1.4
5	$\text{H}_2 + \text{M} \rightleftharpoons \text{H} + \text{H} + \text{M}$	2	16	$\text{H}_2\text{O}_2 (+ \text{M}) \rightleftharpoons \text{OH} + \text{OH} (+ \text{M})$	2.5
6	$\text{O} + \text{O} + \text{M} \rightleftharpoons \text{O}_2 + \text{M}$	2	17	$\text{H}_2\text{O}_2 + \text{H} \rightleftharpoons \text{H}_2\text{O} + \text{OH}$	3
7	$\text{O} + \text{H} + \text{M} \rightleftharpoons \text{OH} + \text{M}$	3	18	$\text{H}_2\text{O}_2 + \text{H} \rightleftharpoons \text{HO}_2 + \text{H}_2$	2
8	$\text{H} + \text{OH} + \text{M} \rightleftharpoons \text{H}_2\text{O} + \text{M}$	2	19	$\text{H}_2\text{O}_2 + \text{O} \rightleftharpoons \text{OH} + \text{HO}_2$	3
9	$\text{H} + \text{O}_2 (+ \text{M}) \rightleftharpoons \text{HO}_2 (+ \text{M})$	1.2	20	$\text{H}_2\text{O}_2 + \text{OH} \rightleftharpoons \text{HO}_2 + \text{H}_2\text{O}$	2
10	$\text{HO}_2 + \text{H} \rightleftharpoons \text{H}_2 + \text{O}_2$	2	21	$\text{H}_2\text{O}_2 + \text{OH} \rightleftharpoons \text{HO}_2 + \text{H}_2\text{O}$	2
11	$\text{HO}_2 + \text{H} \rightleftharpoons \text{OH} + \text{OH}$	3			

combustion products, is employed to demonstrate the propagation of kinetic uncertainty through active subspace. Comprehensive investigations of this flame, such as the detailed comparison between calculations and measurement and the flame stabilization mechanism, etc., have been conducted in [17–19]. In addition, sensitivities to the coflow temperature and chemistry, etc. have been reported by using either divided difference [17–19] or particle-level sensitivity analysis [20]. However, these studies are limited to either the sensitivity with respect to different mechanisms or local sensitivities to individual reactions without accounting for the coupling between the kinetic parameters.

The focus of this study is on the propagation of the kinetic uncertainty to the predicted liftoff height H using active subspace, and the global sensitivities with respect to the kinetic parameters. The flame is simulated using the transported probability density function method (TPDF) in conjunction with the standard k - ϵ model and enhanced wall treatment in Fluent. The constant $C_{1\epsilon}$ is adjusted from 1.44 to 1.6 for better jet spreading rate prediction. The Interaction-by-Exchange-with-the-Mean (IEM) model with $C_\varphi = 2.0$ is employed for micromixing. The In Situ Adaptive Tabulation (ISAT) tolerance is $\epsilon_{\text{tol}} = 6.25 \times 10^{-6}$, which is sufficiently small for ensuring numerical accuracy according to the study in [17]. The coflow temperature is 1045 K if not otherwise specified. The rest of the solver settings and the computational domain are identical to those in [17]. A grid of 22k cells with 50 particles per cell is employed, which ensures grid independence as shown in Fig. 1b.

The Li mechanism consisting of 21 elementary reactions [21] is employed with the temperature independent uncertainty factors being adopted from Konnov [22], as listed in Table 1. The predicted OH contour and mixture fraction profile are shown in Fig. 1, which demonstrates good agreement in the mixture fraction between the experimental and numerical results. As in [14], the liftoff height H is defined as the first axial location normalized by the diameter of the fuel jet, z/D , at which the Favre mean mass fraction of OH reaches a value of

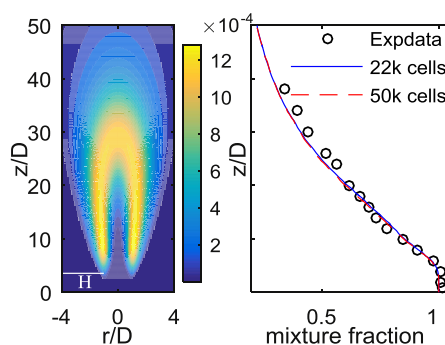


Fig. 1. (a) Contour plot of Y_{OH} from the base case. (b) Profiles of mixture fraction along the axial line from both simulation and experiment.

2×10^{-4} . It is noted that the definition of lift-off height does not affect the conclusions drawn herein. Each TPDF run costs about 2000 CPU-hours using 48 Xeon-E5 processors. It is computationally infeasible to build a 21-dimensional response surface due to the large number of runs needed. Previous budget analysis [18] and sensitivity analysis [23] suggest that flame stabilization is mainly attributed to the auto-ignition process. Hence we first study the active subspace of the ignition delay (IDT) in 0-D autoignition processes at representative conditions of the Cabra flame. These 0-D tests can explore the level of linearity for H in the kinetic parameters space and thereafter the dimension of the active subspace for H in Cabra flame since they share the same dominant physical processes.

4. Results

4.1. Autoignition tests

Wang and Pope [24] have shown that the composition of particles originating from the fuel jet evolves along the mixing line between the jet and coflow compositions before ignition, and the

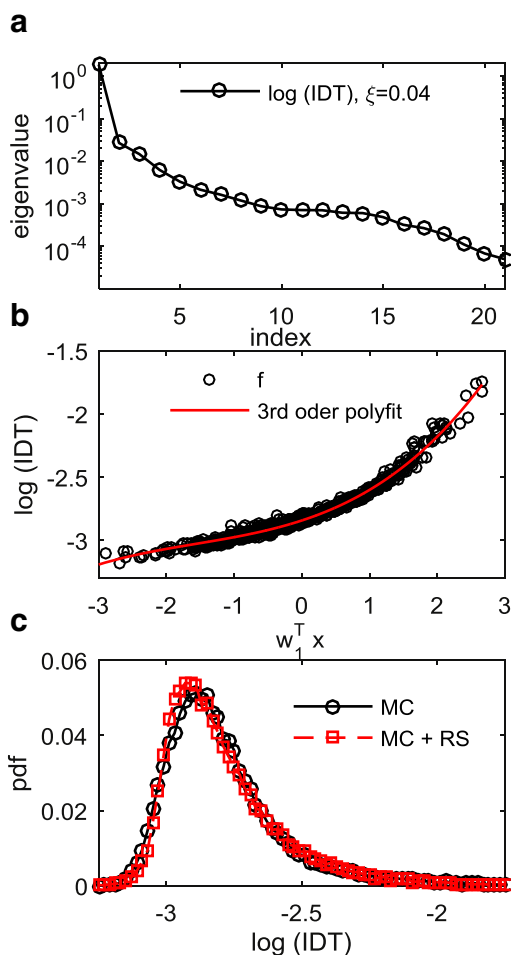


Fig. 2. (a) The eigenvalues, (b) summary plot using 670 samples ($670 = 10 \times 22 \times \log(d)$) with gradient information, and (c) the pdf distribution of IDT[s] using $N = 50,000$ samples.

ignition first occurs near mixture fraction $\xi = 0.04$. Consequently, the composition of $\xi = 0.04$ from the mixing line is chosen as the initial condition for the adiabatic, isobaric autoignition tests. The corresponding temperature is 1015.4 K and the mass fractions are $Y_{\text{H}_2} = 9.9049 \times 10^{-4}$, $Y_{\text{O}_2} = 0.1642$, $Y_{\text{H}_2\text{O}} = 0.0620$ and $Y_{\text{N}_2} = 0.7728$. The gradient of the IDT to the rate constant is computed using finite difference. The IDT in log scale, instead of linear scale, is chosen as the QoI as it tends to be more linearly dependent on variations of the rate constants.

The corresponding eigenvalues estimated using 670 samples are shown in Fig. 2a. It is seen that the first eigenvalue is larger than the second one by two orders of magnitude, implying the existence of a one-dimensional active subspace. This is further confirmed by the summary plot of

Fig. 2b, showing the distribution of IDTs along the active variable, which is the projection of the vector of 21-dimensional input variables onto the one-dimensional active subspace, i.e., $w_1^T x$. The IDTs lie close to a one-dimensional curve and the scattering in the direction orthogonal to the active direction is small. A one-dimensional response surface based on a 3rd order polynomial fitting can be built and is shown as the solid line in Fig. 2b. Then $N = 50,000$ samples are drawn and evaluated using the response surface. The resulting probability distribution function (pdf) of IDT, termed as MC + RS and shown in Fig. 2c, agrees very well with the one from directly evaluating each sample through autoignition integration with Cantera, termed as MC. The differences in the mean and standard deviation of IDT from the response of the two approaches are within 2%. This demonstrates the accuracy of the one-dimensional active subspace in propagating the kinetic uncertainty.

The components of the active direction, i.e., the first eigenvector, are shown in Fig. 3. The magnitude of each component provides a global sensitivity score for the individual reaction. As shown, the most sensitive reaction is R1, which is the major chain branching reaction for hydrogen/air ignition. Other important reactions are those related to HO_2 , i.e., R9 and R11. Note that R9 is a chain termination reaction that inhibits ignition, while R11 is a chain branching reaction that promotes ignition. As such, the components of R1 and R11 have the opposite sign as that of R9. It is found that the active direction almost does not change for the most reactive mixtures of ξ between 0.02 and 0.06, indicating that it is invariant for the reactive mixtures of interest (not shown).

Since it is computationally intractable to evaluate the gradient of the lift-off height H in the Cabra flame, global linear fitting with OLS is employed to identify the active direction. The adequacy of this approach is first investigated for the IDT. The estimated active direction and its error by using different numbers of samples are studied by bootstrapping. It is found that $M = 4d = 84$ samples are adequate for estimating the active direction. As shown in Fig. 3, the relative errors for the large components in magnitude are small, even though the fitting with OLS introduces certain errors (small in magnitude) for insignificant reactions due to the limited samples. Overall, the estimated active direction is very close to the accurate one from Eq. (3) using function gradients with an inner product of 0.99.

4.2. The Cabra flame

Based on the autoignition tests, the lift-off length in log-scale for the Cabra flame is expected to have a one-dimensional active subspace. The $\log(H)$ is assumed to be nearly linearly dependent

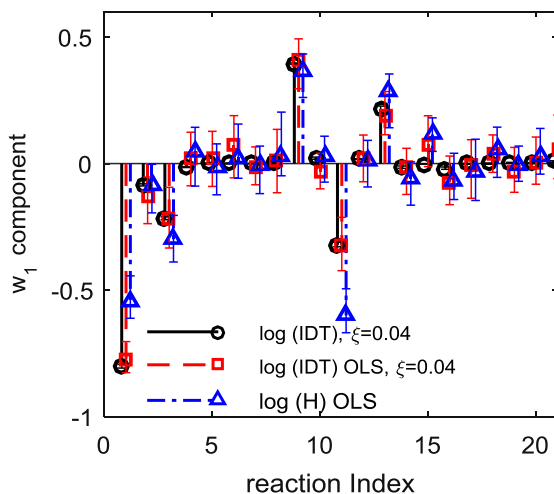


Fig. 3. Components of the first eigenvector for the autoignition tests computed with gradient and OLS. Also shown are the components of the active direction for the liftoff height H in the Cabra flame.

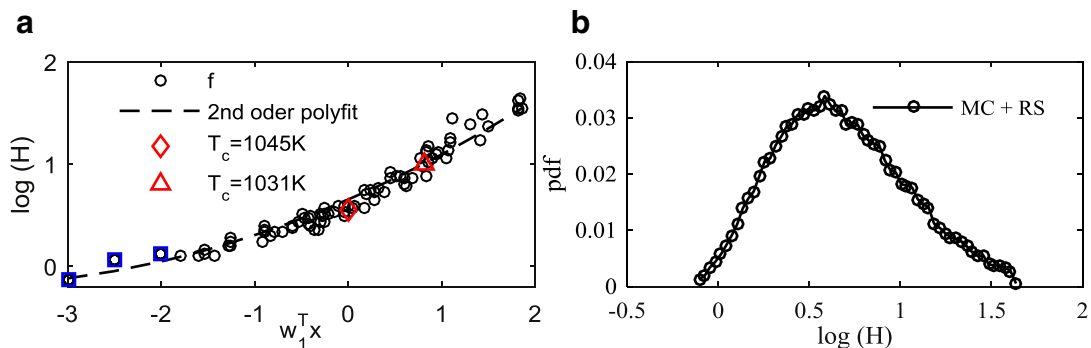


Fig. 4. (a) Summary plot and (b) pdf distribution of $\log(H)$. Blue square symbols in (a) are from three additional runs of the simulation collected to improve the performance of the response surface at the boundary of the parameter space.

on the change of the rate constants, and the active direction is computed using OLS with 84 samples ($M = 4d$). The summary plot is shown in Fig. 4a. The identified one-dimensional active subspace captures most of the variations of H . Similar to the case of IDT, the small variation in other directions results from the error in the estimated active subspace due to insufficient number of samples. The response surface, based on second-order polynomial fitting is also shown in Fig. 4a. The R-square value of the fitting is 0.97, which suggests that the fitting error is sufficiently small for the present application. Then 50,000 samples are drawn and evaluated using the second-order polynomial fitting. The resulting pdf of $\log(H)$ is shown in Fig. 4b. The mean of $\log(H)$ is 0.67 or $H = 4.6$. The 95% confidence interval of H is [1.1, 28.3], which covers the measured 10D.

The components of the active direction in Cabra flame are shown in Fig. 3. Compared to the ones of IDT, the sensitivities to the reactions R11 and R13 are promoted while R1 is relatively weakened in the Cabra flame. Both reactions R11 and R13 are the major consumption reactions of HO_2 . According to the budget analysis in [18], the diffusion term leads to the presence of high concentration HO_2 ahead of the flame stabilization zone, which accounts for the promoted sensitivity of the HO_2 consumption reactions. It can also explain the promoted sensitivity of R3. However, given the uncertainty associated, the conclusion is weak, as the change is less significant than R11 and R13. Nevertheless, the top sensitive reactions, e.g., R1, R9, and R11 remain the same, and the active directions between H and IDT are quite similar to each other, with an inner product of 0.91. This therefore

suggests that one can first study the cheap test cases to estimate the dimension and large components of the active subspace for the expensive turbulent flame simulations, if the test cases and the turbulent flame simulations share the same dominant physics. The similarity in dominant physical processes can be analyzed via various computational diagnostic tools such as budget analysis [18] and Lagrangian tracking [24] referred to above. The number of required runs of the model to accurately estimate the active subspace can also be estimated in the test cases. In addition, one can identify the unimportant parameters based on the test cases, and exclude them when identifying the active subspace for the expensive model. This will result in fewer samples needed for the expensive model, as M is at least linearly increases with the number of parameters. However, as shown in Fig. 3, the insensitive reactions for IDT can be promoted by the diffusion process in the Cabra flame. To be conservative, a sufficiently small threshold should be chosen to determine the insensitive reactions. Since the number of parameters for the hydrogen mechanism is relatively small, determination of the threshold is unnecessary for the present work; and is subject to future study for larger mechanisms.

Previous studies [19,20] have also shown that H is very sensitive to the co-flow temperature T_c , such that a decrease of 10 K in T_c can double H . The change of T_c can lead to the change of reaction rates ahead of the flame zone. It can also change the maximum temperature in the flame zone as well as the relevant characteristics of the flame, such as the flame speed. To study how T_c affects H , a simulation under $T_c = 1031$ K is performed. The T_c of 1031 K is chosen as the predicted $H = 9.75$ is very close to the measured 10D. Then the effect of different T_c on the rate constant under $\xi = 0.04$ is scaled to the changes of the pre-factor A , and is further scaled to the input parameter x . Specifically, the rate constants are evaluated at the temperatures corresponding to the mixture fraction of 0.04 from the mixing line, i.e., 1015.4 K for $T_c = 1045$ K and 1002 K for $T_c = 1031$ K, respectively. Previous Lagrangian analysis [24] shows that the composition state is attained to the mixing line before ignition, thus this characteristic temperature can represent the global influence of the co-flow temperature on the flame. The corresponding centered and normalized x and H , shown in Fig. 4a, demonstrate excellent consistency with the active subspace for the rate constants. This suggests that the effect of T_c is mainly through changing the rate constant ahead of the flame zone. It also questions the common approaches to match H by adjusting T_c . To make further judgment about the major uncertainty source, one can conduct the *inverse* problem mentioned in the introduction to reduce the uncertainty in the mechanism. As the active directions for H

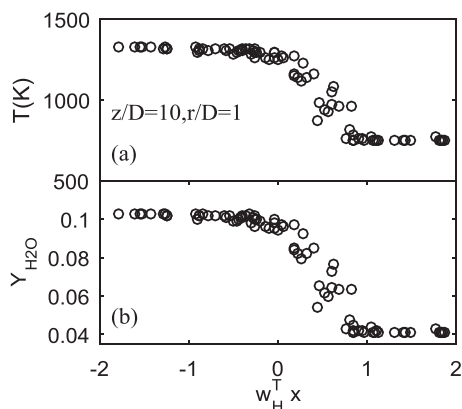


Fig. 5. Summary plot of temperature and $Y_{\text{H}_2\text{O}}$ against the active direction of $\log(H)$.

and IDT are similar, a small number of experimental datasets of IDT can significantly reduce the uncertainty in the predicted IDT as well as H .

It is also interesting to study the active subspace of the temperature and species profiles. However, these profiles tend to be extremely nonlinear and the OLS is not suitable here. While it is infeasible to compute their active subspace with the collected samples above, we can easily check whether the active subspace for the liftoff height can explain the variations of these profiles. The summary plot of temperature T and major product of H_2O from the location $z/D = 10$, $r/D = 1$ against the active direction of H is presented in Fig. 5. It is seen that the active subspace of H can capture the major trend of T and $Y_{\text{H}_2\text{O}}$. Compared to the variation of H in Fig. 4a, \bar{T} and $Y_{\text{H}_2\text{O}}$ only change when $z/D = 10$, $r/D = 1$ is close to the flame stabilization zone, i.e., H is close to 10. Therefore, the species profiles and liftoff height H are most likely to share the same active subspace and be correlated in terms of the response to the kinetic parameters. Such similarity can be used to estimate the uncertainty of the species profiles.

5. Conclusions

The active subspace approach is applied to propagate 21 kinetic parameters to the liftoff height H in the TPDF simulation of the Cabra H_2/N_2 lifted flame. We first identified a one-dimensional active subspace based on 84 runs of the simulation. Then a one-dimension response surface is built. Finally, the distribution of H is characterized by evaluating 50,000 samples using the response surface, showing that kinetic uncertainty alone is large enough to account for the discrepancies between the measurements and simulations.

The present work demonstrates the capability of active subspace in revealing the effect of flow-chemistry in turbulent combustion simulations. The identified active subspace for H is compared with that for the ignition delay under flame conditions, and they are generally similar to each other with the most sensitive reactions being the same. The difference reveals that the sensitivity of the HO_2 consumption reactions is promoted due to the diffusion process in the Cabra flame. As the results indicate that the diffusion process alters the sensitivities of the HO_2 consumption reactions, future work might include transport parameters as an additional uncertainty source to investigate the effect of flow-chemistry interaction more conclusively.

Compared to previous work on the uncertainties of the operating conditions [12], the kinetic uncertainty has higher dimensions and is more challenging. In addition, the simple zero/one-D simulations share the same kinetic uncertainty inputs with the turbulent combustion simulations, and as such are used to estimate the active subspace in turbulent flames. The identification of active subspaces via inexpensive surrogate models is a potential effective solution for expensive turbulent combustion simulations with large mechanisms or strongly nonlinear response. The approach is open to other types of flame and various turbulent combustion models.

Acknowledgments

This work was supported by the National Natural Science Foundation of China Nos. 91441202 and 51476087.

References

- [1] M. Frenklach, H. Wang, M.J. Rabinowitz, *Prog. Energy Combust. Sci.* 18 (1992) 47–73.

- [2] H. Wang, D.A. Sheen, *Prog. Energy Combust. Sci.* 47 (2015) 1–31.
- [3] K. Braman, T.A. Oliver, V. Raman, *Combust. Theory Model.* 17 (2013) 858–887.
- [4] B.D. Phenix, J.L. Dinaro, M.A. Tatang, et al., *Combust. Flame* 112 (1998) 132–146.
- [5] M.T. Reagan, H.N. Najm, R.G. Ghanem, O.M. Knio, *Combust. Flame* 132 (2003) 545–555.
- [6] I.G. Zsély, J. Zádor, T. Turányi, *Proc. Combust. Inst.* 30 (2005) 1273–1281.
- [7] D.A. Sheen, X. You, H. Wang, T. Lovås, *Proc. Combust. Inst.* 32 (2009) 535–542.
- [8] M.J. Davis, R.T. Skodje, A.S. Tomlin, *J. Phys. Chem. A* 115 (2011) 1556–1578.
- [9] G. Esposito, B. Sarnacki, H. Chelliah, *Combust. Theory Model.* 16 (2012) 1029–1052.
- [10] P.G. Constantine, E. Dow, Q. Wang, *SIAM J. Sci. Comput.* 36 (2014) A1500–A1524.
- [11] W. Ji, J. Wang, O. Zahm, et al., *Combust. Flame* 190 (2018) 146–157.
- [12] P.G. Constantine, M. Emory, J. Larsson, G. Iaccarino, *J. Comput. Phys.* 302 (2015) 1–20.
- [13] M.E. Mueller, G. Iaccarino, H. Pitsch, *Proc. Combust. Inst.* 34 (2013) 1299–1306.
- [14] R. Cabra, T. Myhrvold, J.Y. Chen, R.W. Dibble, A.N. Karpetis, R.S. Barlow, *Proc. Combust. Inst.* 29 (2002) 1881–1888.
- [15] R. Tipireddy, R. Ghanem, *J. Comput. Phys.* 259 (2014) 304–317.
- [16] P.G. Constantine, P. Diaz, *Reliab. Eng. Syst. Saf.* 162 (2017) 1–13.
- [17] A. Masri, R. Cao, S. Pope, G. Goldin, *Combust. Theor. Model.* 8 (2004) 1–22.
- [18] R.L. Gordon, A.R. Masri, S.B. Pope, G.M. Goldin, *Combust. Theory Model.* 11 (2007) 351–376.
- [19] R.R. Cao, S.B. Pope, A.R. Masri, *Combust. Flame* 142 (2005) 438–453.
- [20] Z. Ren, S.B. Pope, *Proc. Combust. Inst.* 32 (2009) 1629–1637.
- [21] J. Li, Z. Zhao, A. Kazakov, F.L. Dryer, *Int. J. Chem. Kinet.* 36 (2004) 566–575.
- [22] A.A. Konnov, *Combust. Flame* 152 (2008) 507–528.
- [23] S.M. Mir Najafizadeh, M.T. Sadeghi, R. Sotudeh-Gharebagh, D.J.E.M. Roekaerts, *Combust. Flame* 160 (2013) 2928–2940.
- [24] H. Wang, S.B. Pope, *Combust. Theory Model.* 12 (2008) 857–882.